EPJ Photovoltaics **17**, 4 (2026)
© B. Jaeckel et al., Published by EDP Sciences, 2026
https://doi.org/10.1051/epjpv/2025024

Available online at:
www.epj-pv.org

Special Issue on 'EU PVSEC 2025: State of the Art and Developments in Photovoltaics', edited by Robert Kenny and Carlos del Cañizo

ORIGINAL ARTICLE OPEN ACCESS

Characterization and analysis of reverse breakdown voltage onset of solar cells with different cell architectures

Bengt Jaeckel[1,*], Jens Froebel[1], Matthias Pander[1], Andreas Maixner[2], and Hamed Hanifi[2]

[1] Fraunhofer Center for Silicon Photovoltaics CSP, Halle (Saale), Germany
[2] AESOLAR, Messerschmittring 54, Koenigsbrunn, Germany

Received: 30 June 2025 / Accepted: 15 November 2025

Abstract. In 2016 Passivated Emitter and Rear Cell (PERC) solar cells started to dominated the PV industry as cell technology. Since 2023, the prices of Tunnel Oxide Passivated Contact (TOPCon) and Heterojunction (HJT) solar cells have become lower, leading to a strong decline in PERC technology till today. TOPCon is now (2025) the mainstream cell technology, while HJT and BC (Back Contact) cells are gaining market share. All technologies feature different cell sizes and quantities, resulting in higher voltages, currents and different reverse characteristics compared to PERC. One major challenge in integrating these new technologies into existing module designs is understanding the reverse bias behavior of solar cells to avoid excessive overheating of partially shaded cells. Evaluating this behavior is crucial for the durability and reliability of PV modules when fully / partially shaded. In such scenarios, shaded cells operate as a load, altering current flow. If the voltage of the series-connected cells exceeds the reverse breakdown voltage of a single cell, that cell can undergo electrical breakdown in reverse bias, consuming energy produced by the other cells. Excessive heat generation due to defects can lead to hot-spots, melting of encapsulants or solder, glass breakage, and even fires. Given the trend toward larger cells (G12, M10) and higher cell quantities (more than 20) for increased module power, a reevaluation of the breakdown behavior of solar cells is urgently needed. To properly understand the behavior of new solar cell technologies in the market, all major architectures were evaluated. Mini-modules were manufactured with the different cell architectures and characterized in forward and reverse bias. The cells/mini-strings were measured at irradiance levels from 100 to 1300 W/m^2 in the 1st quadrant all the way to reverse breakdown in the 2nd quadrant. This was especially challenging for HJT and TOPCon cells as they have a pronounced hysteresis effect in the 1st quadrant. However, neither TOPCon nor HJT shows an accountable hysteresis in the reverse breakdown region. As both technologies are bifacial, the behavior is not significantly different between front and rear side. Besides the higher breakdown voltages, −44 to −49V and around −30V for TOPCon and HJT, respectively, their irradiance dependent reverse current increase is compared to PERC low to very low. The results of TOPCon and HJT solar cells show a promising reverse breakdown behavior even with strings with higher number of solar cells under full and potentially also under partial shading conditions.

Keywords: Hot-spot / partial shading / reverse bias / reliability / energy loss

1 General introduction

In recent years, module efficiencies have significantly increased and module interconnections have been substantially further developed starting from the introduction of 3 busbar cells around 2010 to the today's standard of 16 and more wires [1]. Moreover, the module concepts changes from 3×20, some times 3×24, cells in series to a serial/parallel configuration in modern half-cut cell modules with 2 submodules in parallel with 3 strings containing 18 to 26 cells leading to 108 to 156 cells in a PV-module. The main module efficiency increase is related to the efficiency improvements resulting from the introduction of new cell concepts starting at Al-BSF to PERC on *p*-type silicon. Today's TOPCon, HJT, and Back-Contact (BC) concepts are mainly based on *n*-type silicon [1].

These cell enhancements lead to quite different cell IV-characteristics in reverse bias. Reverse bias typically occurs if the full or parts of a solar cell are shaded, forcing the cell into reverse bias and acting as an energy "consumer", not a producer. This leads to localized or areal heat generation in the shaded solar cell. The type of heat generation depends on the reverse current flow paths

* e-mail: bengt.jaeckel@csp.fraunhofer.de

This is an Open Access article distributed under the terms of the Creative Commons Attribution License (https://creativecommons.org/licenses/by/4.0), which permits unrestricted use, distribution, and reproduction in any medium, provided the original work is properly cited.

and localization. Different mechanisms are known and will lead to different localized heat generation [2–13] processes such as edge insulation (shunting along cell edge), impurities and grain boundaries (can be everywhere in the cell) and areal reverse breakdown of the pn-junction of the solar cell. That also leads to the observation that multi-crystalline solar cells are more prone to reverse breakdown compared to mono-crystalline cells with the same fundamental cell architecture. The available power to generate heat depends on the electrical circuitry of the PV-module, reverse breakdown behavior of the (shaded) solar cell(s), irradiance and will be briefly reviewed in sub Section 1.3.

The term reverse breakdown is used in here to define the strong onset of current increase. As the experiments were done it was intended to not damage the cells during testing. However, if the pn-junction fully breaks down and high currents flow permanent damage to the cell occurs. As mentioned in the experimental section care was taken to not permanently damage the cell.

1.1 Reference to standards

For type-approval testing of PV-modules a hot-spot test is performed. The test procedure is described in MQT 09 (Module Quality Test) of IEC 61215-2 [14]. Different types of reverse characteristics of cells are considered, together with different module layouts. However, during the development of the current hot-spot test (MQT 09) of the IEC 61215-2 s [14], findings were considered that date back significantly to before 2021 [15–23]. Even in the latest 2021 edition, no significant changes were made to the hot-spot test for crystalline modules, especially with regard to the pass-fail and test duration criteria.

Higher output power of modules was not only achieved by higher solar cell efficiencies. New module concepts were also derived to increase output power per square-meter by new interconnection techniques such as gapless with standard cell interconnection or shingling approaches [24]. Shingling can be done either as a linear configuration, but also as a matrix concept. Their response of partial shading highly dependence on the electrical cell circuitry within the PV module [25–28]. At the time of the 2016 edition, there were already the first half-cell module concepts on the market, which were generally conservatively designed with 20 cells per bypass diode. PV-modules for large power plant application have quite often up to 156 cells, resulting in 26 cells per bypass diode. Driving force is mainly cost reduction and the rare occurrence of partial shading is accepted which is compliant with the current version of the hot-spot test and achieving type approval and CE marking for the European market.

1.2 Relevance for new applications

For most large scale ground mounted systems the test is sufficient for most cell and module concepts as it considers partial shading as a fault-case scenario that only occurs once. However, in the use-case of C&I (Commercial and industrial), BaPV (Building attached PV) and BiPV (Building integraded PV) application the trend is that the partial shading is accepted in terms of partially reduced energy yield and it is assumed that the durability of the module against this repeated "faulty" shade scenario is covered. Unfortunately, this is not the case and will be an increased safety risk in the future, as such PV applications are growing strongly worldwide [29]. Even if MQT 09 is performed in the "extended" version, there is only slight concern that something happens with the module since the test duration is at maximum 5 h. Additionally to the partial shading modules mounted close to a roof or a facade will have generally higher operating temperatures. This is tried to be partially covered for setting testing conditions by the current version of IEC TS 63126 [30].

Assuming a shading scenario on a roof that occurs daily throughout the year and tends to appear for 1 h per day, results in about 7000 h of extra localized heating in a typical service live of 20 yr. A test protocol to cover parts of this was proposed in [31] and is currently discussed in the IEC TC 82 WG2 group as "severe hot-spot-Test". It is important to note that partial shading is not any more a faulty situation, it is an accepted use-case scenario. Tests from different groups [31–33] have shown that cells from today's modules can easily reach temperatures above 200°C, well above lamination temperature and also above the melting point of the solders used.

1.3 Technical background of (partial) shading

The extent to which a shaded cell generates heat depends on the operating point of the module and the operating point of the shaded cell. This is schematically shown in Figure 1. Maximum heating can be achieved, if all power of the fully irradiated cells (n-1, where n-1 can be e. g. 17, 19, 23) can be used for (locally) heating the shaded cell. Voltages and currents have to match. If the shaded cell's reverse breakdown voltage is too high (orange and green curves), only a small fraction − if any − of the generated power can be dissipated. Such configurations are "hot-spot"-safe with the assumption of a fully shaded cell. For partial shading the power will increase and cell temperature can and will increase compared to non-shaded cells.

A distinction must be made between local and extended area-wide heating. Older cell generations, typically Al-BSF (Aluminum back surface field), often exhibited local shunts [10,22] caused by impurities (e.g., poor wafer material) or manufacturing process variations [34–36] leading often to very localized defects and result in very localized heating spots (name: hot-spot!). Accordingly, cells were and are sorted based on their power and there reverse blocking characteristics, resulting in different module constructions with a varying number of cells per bypass diode (12, 16, 20, later 24 cells/bypass diode). The use of newer cell architectures and mono-crystalline material lead to a significant increase in reverse breakdown voltage for most cell architectures leading to the newer phenomena of area-wide heating. Here typically most heat is generated if a cell is partly shaded. The still illuminated area shows highest temperature when around half of the solar cell is shaded

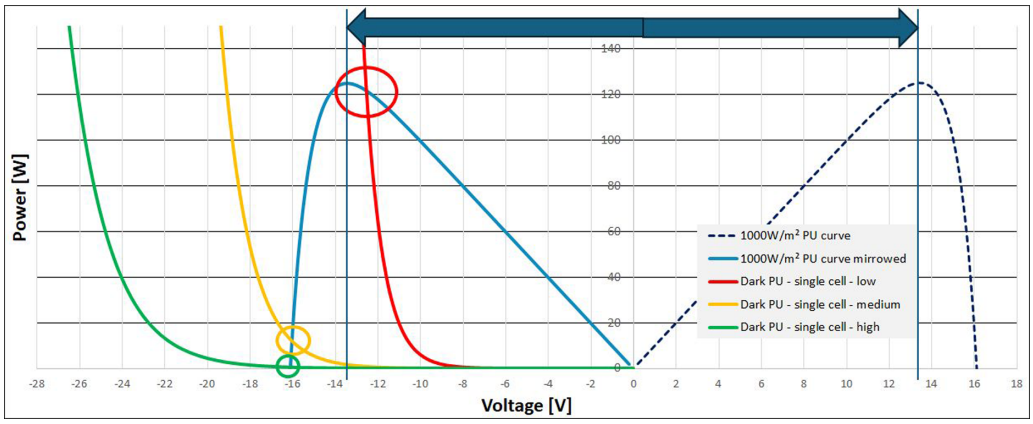

Fig. 1. Schematic PU curve for an unshaded string (n−1 cells, dotted line) on the right side and mirrored to the left (blue line). Red, orange and green represent PU curves of three different cell types with different reverse breakdown behavior in dark condition. The intersections represent points with maximum power transfer between unshaded power generating cells (n−1) and power dissipating shaded cell.

[31,33]. Operation point of the partial shaded cell is in reverse but irradiance dependence of the cell must be considered − see next paragraphs.

Additionally cell-cutting processes can also have an impact on cell's reverse breakdown behavior [8]. However, the development focus in modules primarily lies on performance in forward/illuminated IV-characteristics, and the properties important for shading scenarios in reverse bias are often not specifically investigated.

Figure 1 assumes a fully shaded cell and n-1 cells acting as power source. However, this scenario is very unlikely. More likely are shading scenarios with 20–80% coverage of a cell. This results in parts of the cell being illuminated, whereas another part is operated in the dark and the full cell is biased in reverse.

As shown by several groups [21,31,33,37,38] partially shaded cells can heat up in the unshaded area to temperatures significantly above 150 °C, even above 200 °C. Under these conditions the non-illuminated area basically can be neglected for current transfer and reverse bias heating as the generated current of the n-1 non-shaded cells flows through the unshaded cell part. Different irradiance level scenarios of typical PERC cells (see e.g. Fig. 6b) with short circuit correction are illustrated in Figure 2 for a fixed temperature. It must be noted that reverse breakdown voltage is also temperature dependent and typically decrease with increasing temperature and making therefor heating more severe. Further work is currently done on this topic to complement the work done on older cells e.g. in References [5].

Modeling of reverse breakdown of cells is done for decades [2,7,11,13] and is improved for better predicting moduleâ€™s shading response. The relevance and severity of impact of illumination on reverse breakdown behavior was presented e.g. by Clement in 2021 [37]. This paper builds up further data and understanding to this very relevant topic.

New cell and module technologies come with larger cells, higher open-circuit voltage and short-circuit current, combined with a higher number of cells in series in utility scale large size PV modules. This makes a revisit of reverse breakdown as a function of cell technology and illumination necessary. The reverse breakdown behavior analysis and characterization can determine the quantity of cells and evaluates the risk of hot-spots in the presence of partial shading in dependence of the used cell architecture.

1.4 Approach

To better understand the impact of new cell concepts on excessive heat generation under full or partial shading, five cell types commonly used over the past 15 years were investigated: Alâ€‘BSF (Aluminium back surface field), PERC (passivated emitter and rear cell), TOPCon (tunnel oxide passivated contact), HJT (heterojunction), and (I) BC ((interdigitated) backâ€‘contact) cells. Based on the number of serial interconnected solar cells a certain voltage is available to drive a cell in reverse bias conditions. This number of cells has changed from typical 20 cells per bypass diode to quite often at least 24 cells per bypass diode increasing available voltage and power for heat generation.

The breakdown behavior of the cell is essential to the resulting (local) heat generation in a shaded cell. Other studies have shown, that the reverse characteristic of solar cells is very different for each cell architectures, and amount of illumination [37–41]. To optimize a module design in terms of full and partial shading resistance and long-term durability the properties of each cell type must be known and considered for the electric circuit designs to incorporate bypass diodes for module protection and to improve energy yield.

Besides the knowledge of each cell type architecture reverse breakdown behavior influencing factors such as cell manufacturing deviations must be considered. That the manufacturing process of the solar cell can have a significant impact was e. g. shown in [35,36] for PERT (PERC like structure) on *n*-type material and for PERC-like structure on *p*-type material. In general, non optimal process conditions lead to a significant decrease in reverse breakdown characteristics or at least to a significant increase in reverse leakage current.

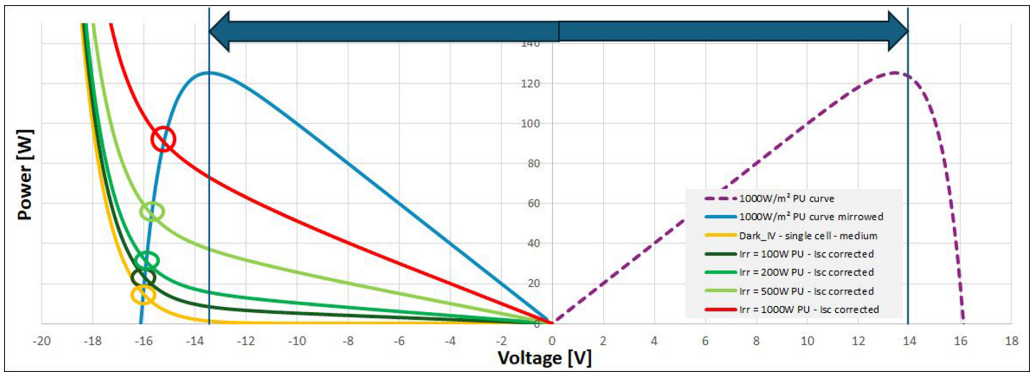

Fig. 2. Schematic PU curve for an unshaded string on the right side and mirrored to the left (to show crossing points). Colored from Orange (same as "medium" in Fig. 1) of a dark PU to red a partially shaded cell with different shading ratios. The intersections represent maximum power transfer between unshaded power generating cells and power dissipating shaded cell.

Additionally the "daily-use-case" scenario is currently changing. While in the past PV modules were installed mainly shade free due to there cost, today more and more installations accept partial shading of the modules on a daily basis. Therefore, the risk of having hot-spot heating events and potential damage to the PV module is significantly increased and is the worst case for the building or infrastructure.

Irradiance, temperature and variations in cell processing (size, manufacturing year) will be presented and discussed herein with the focus on irradiance dependence.

2 Experimental setup

The aim of the study was to evaluate the IV-characteristics of Al-BSF, PERC, TOPCon, HJT and IBC solar cells in reverse and forward bias directions to evaluate the risk of hot-spot and damages in new cell technologies and (re)define a limit on the number of solar cells in a serial interconnected solar cell string. Understanding the cell's behavior under partial illumination in reverse operation is most relevant for today's shading test and its relevance to real world operation. The focus herein is on irradiance dependence. This is not the only parameter to consider. Each cell technology also does have a temperature dependence in reverse direction, similar to the temperature coefficient in the 1st-quadrant, often lowering breakdown voltage [42].

To achieve this mini-modules for each cell technology with single or multiple solar cells and different cell architecture (Al-BSF, PERC, TOPCon, HJT and IBC) were fabricated with various designs to mimic more closely their normal use in full size PV modules. However, this does not have an impact on reverse breakdown behavior only on absolute current values. Contacts to the cells were made such that 4-probe measurements can be done to reduce impact of contacting resistance. The mini-modules are characterized with a A+A+A+ HALM Flash tester, utilizing long-pulse (up to 150ms) testing protocols, including multi-flash for hysteresis reduction and wide voltage range measurements. HALM's electronic load can perform four-quadrant measurements allowing to measure reverse and forward directions of the solar cells in one IV-curve sweep.

TOPCon and HJT solar cells have shown significant hysteresis behavior and a multi-Flash approach is needed to measure such cells correctly. The IV-characteristics were typically determined in an irradiance interval of 100 $\mathrm{W/m^2}$ starting at 100 $\mathrm{W/m^2}$ to 1300 $\mathrm{W/m^2}$ at 25 °C. The irradiance levels were achieved while tuning the light source intensity and for very low levels a neutral density filter was utilized to keep the spectrum close to AM 1.5.

Electroluminescence images were taken for control measurement to check for defects – prior and after reverse biasing during the IV-curve sweeps. No damages were found during the IV-curve collection of the data for this paper.

TOPCon technology is the main stream cell architecture of 2025. For implementation in current modules more information was needed to be collected. Therefore, two batches and several TOPCon cells were measured in detail to also see any impact on cell manufacturing date / batch on reverse bias behavior 3.3 including their bifaciality.

3 Results

3.1 Al-BSF cells

AL-BSF serves as a baseline as most module designs are still based on experience with this technology, in particular the conditions and criteria of the hot-spot test in IEC 61215-2 [14]. Al-BSF cells were often made from multi-crystalline material and this material was typically more sensitive to reverse bias induced localized heating due to impurities and the influence of grain boundaries within the wafer structure [8,10]. The sample used herein was from multi-crystalline material with 3 busbars as shown in Figure 3. The typical crystalline pattern is clearly visible in the EL image. This cell type based on his partly worse reverse characteristic, will be used as reference, since it served also as base for the development of the current hot-spot test.

Figure 4a shows the full set of taken IV-curves at 25 °C. The setting was such that the full forward direction from Isc and Voc could be measured accurately. Additionally the reverse setting was set to the point where breakdown occurs. During measurement of the IV-curves from dark to

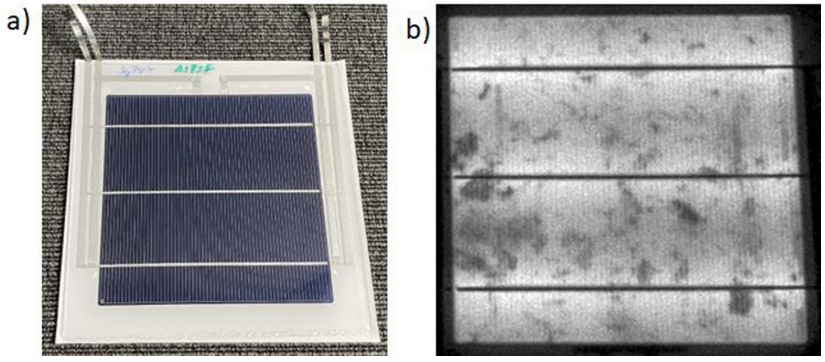

Fig. 3. Al-BSF multi-crystalline silicon solar cell with 3 busbar cell, manufactured around 2010, a) photo with 4-point contacts, b) corresponding EL-image where the typical multi-crystalline structure can be seen.

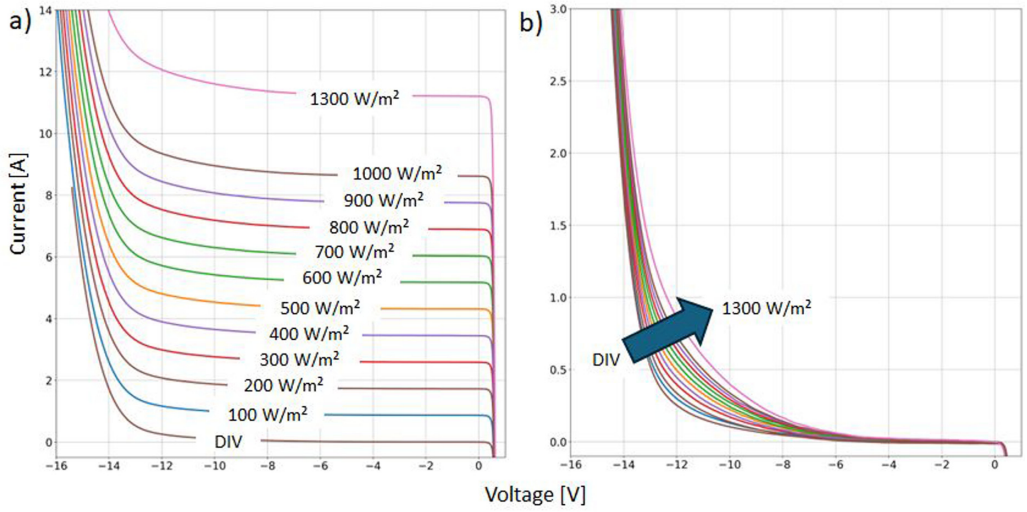

Fig. 4. a) IV-curves taken at 1300W/m^2 and from 1000W/m^2 to dark-IV in 100W/m^2 steps of Al-BSF multi-crystalline cell from Figure 3. b) same IV-curves but always moved by Isc of correlated intensity. Reverse breakdown occurs at around −14V as expected for that solar cell type. A slight irradiance dependence is visible at voltages lower than −5V.

1300 W/m^2 slight adjustments were needed in reverse direction to fully measure the breakdown. For these measurements the cells were not shaded at all. This procedure was utilized throughout the paper for all technologies.

To better illustrate the irradiance dependence from each curve the current at Isc was subtracted. The curves are displayed in Figure 4b. In the range from −5 V to breakdown (14 V) a slight additional increase in reverse current is visible as function of irradiance, indicated by the arrow.

3.2 PERC cells

Until about 2023 PERC technology was the main cell architecture for solar cells. As production of that type of cell started about 2012 there is basically a full decade of manufactured products in the market. From this also a lot of experience was gained, including the findings from [31,33] that PERC cells can achieve significant high temperatures while being partially shaded. Temperatures of more than 200 °C were reported which is higher than lamination temperature and solder melting, rising concerns about long-term reliability. Additionally, the transition from full to half-cells was done during the PERC era.

To cover the transition from full to half cells and the long history of PERC two cells were investigated. One full 5 a)/b) and half 5 c)/d) cell with 5 and 9 busbars, M3 and M6 format, respectively. As can be seen in the EL-images no major observations with respect to VDE-SPEC 90031 [43,44] can be seen. This is important to check that the measured reverse breakdown is representative of cell technology and not of defects such as dark spots or not perfect edge insulation.

Figure 6 shows the IV-curves taken for the full cell and Figure 7 for the half cell. The full cell is manufactured around 2020, the half is around 2024 representing a further development of the cell architecture through-out the years.

The fundamental IV-curve behavior did not change. As the half cell is significant smaller the current itself is lower (note the different scaling in the figures), however, the current density increased slightly over the years.

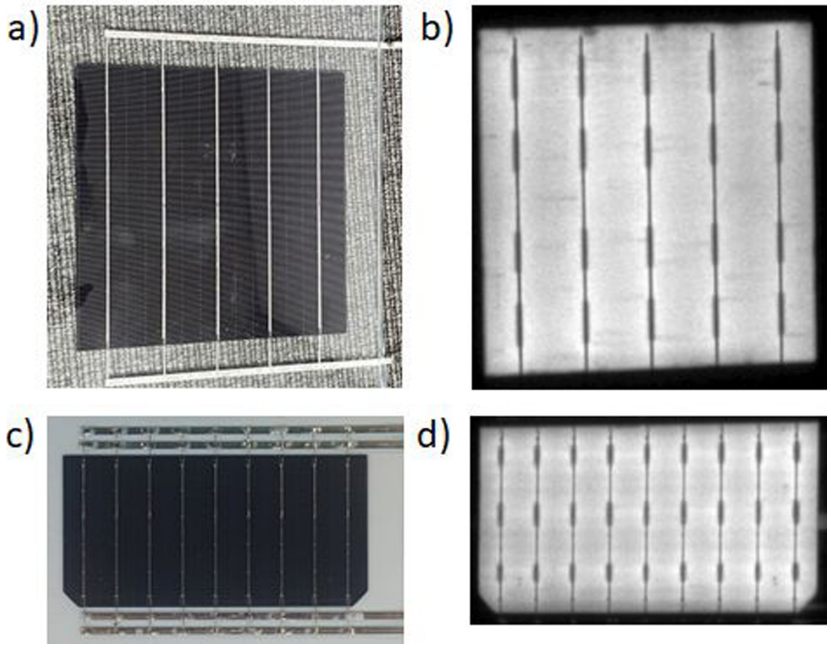

Fig. 5. PERC mono-crystalline silicon solar cell with 5 busbars ((a), b), manufactured around 2020) M3 format, and 9 busbars (c), d), manufactured around 2024) M6 format, a)/c) photo of cells with contacts, b)/d) corresponding EL-image showing no defects, except some finger interruptions.

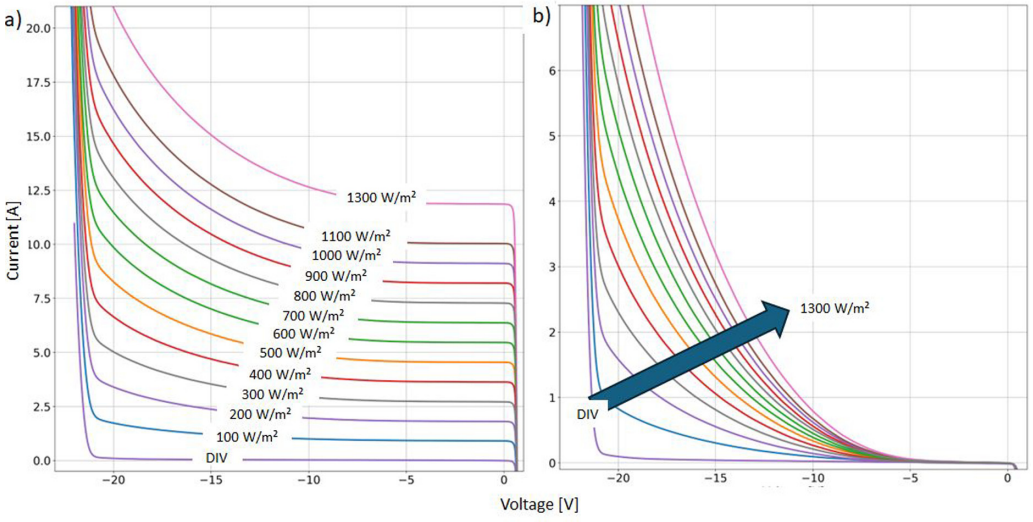

Fig. 6. a) IV-curves taken at 1300W/m^2 and from 1100W/m^2 to dark-IV in 100W/m^2 steps of a 5 busbar PERC mono-crystalline full cell from Figures 5a, 5b. b) same IV-curves but always moved by Isc of correlated intensity. Reverse breakdown occurs at around −22V as expected for that solar cell type. A strong irradiance dependence is visible at voltages lower −5V compared to the one from Al-BSF in Figure 4; note the different y-axis scaling.

Comparing the shape of Figures 6b and 7b no major difference can be seen. The dark IV-curve seems to be a little more "cornery" for the full cell and the half cell is more "round". The relative change or better the dependence on irradiance between the two cell geometries is basically identical.

In the range from −5 to breakdown (22–24V) a strong additional reverse current is visible as function of irradiance, indicated by the arrow. The newer half cell has a little higher reverse breakdown (by 1–2V) voltage.

3.3 TOPCon cells

TOPCon cell architecture entered the market around 2021 and is the main architecture today (2025) [1]. To cover the development of the cell technology a more early cell from late 2023 and from mid 2024 were measured. That such cells can show modification in their behavior is e.g. visible in there efficiency increase, but also in their sensitivity towards UVID [45–48]. To cover this the two cells were selected by year of manufacturing, unfortunately, their UVID sensitivity is not known.

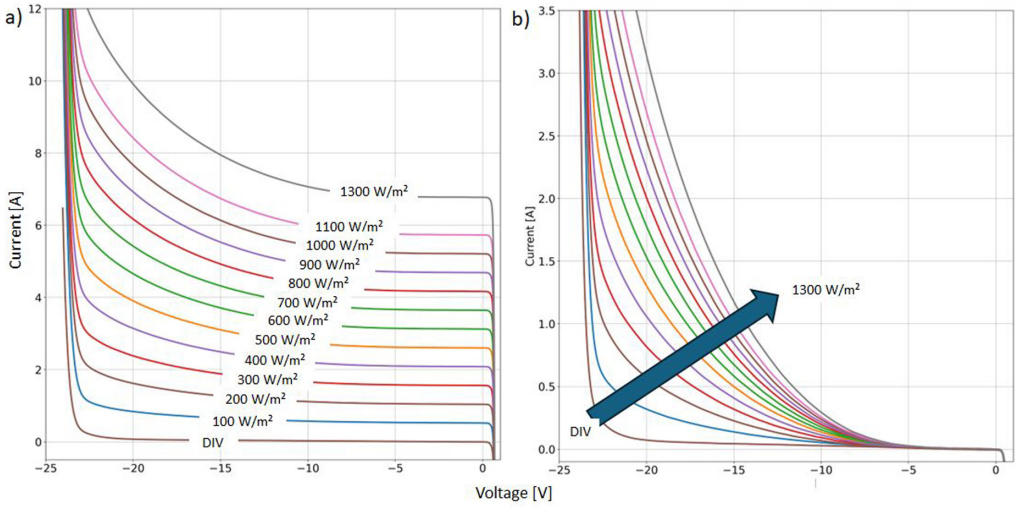

Fig. 7. a) IV-curves taken at 1300W/m^2 and from 1100W/m^2 to dark IV in 100W/m^2 steps of a 9 busbar PERC mono-crystalline half-cut cell from Figures 5a, 5b. b) same IV-curves but always moved by Isc of correlated intensity. Reverse breakdown occurs at around −23V as expected for that solar cell type. A strong irradiance dependence is visible at voltages lower than −5V compared to the one from Al-BSF in Figure 4; note the different y-axis scaling.

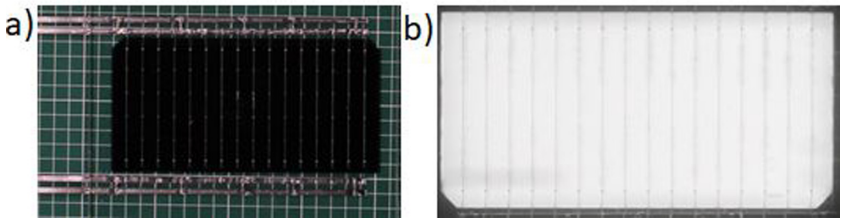

Fig. 8. TOPCon mono-crystalline silicon solar cell with 16 busbars manufactured in late 2023 with M10 format. a) photo of cells with contacts, b) corresponding EL-image showing no defects, except some minor finger interruptions.

Additionally, TOPCon cells present two further aspects to consider. First, they exhibit hysteresis in IV curve measurements when the sweep is performed too quickly (in the 10 ms range). Second, they are bifacial. This raises two questions: do the front and rear sides perform similarly, and does hysteresis influence the results for reverse-bias behavior?

The cell used for the hysteresis investigation is seen in Figure 8 where no major observation can be seen. On the left lower side in the EL-Image (b) there is a little contacting issue (darker gray), but this is a "surface" issue, not a bulk issue that modifies reverse breakdown behavior.

Figure 9a shows the IV-curves taken from the front and rear at 1000W/m^2, 200W/m^2 and in the dark (DIV) in Isc–>Voc and Voc–>Isc direction. The difference between front and rear side efficiency is as expected for this type of bifacial cell. The hysteresis in the first quadrant is marked in the image. Isc–>Voc shows a lower fill factor, and Voc–>Isc a significant higher fill factor here >100%! This was expected for the first quadrant. Although the PV relevant first quadrant measurement shows a hysteresis effect, the reverse bias side does not and the curves are overlaying very well (see Fig. 9a). By subtracting Isc current (Fig. 9b) only a slight difference is visible between front and rear side and as function of irradiance (see next in more detail). Based on these results the full irradiance reverse breakdown IV-characterization of that cell type was done only in Isc–>Voc direction and the lower fill factor is tolerated as the power (1st quadrant) is not the focus of this investigation.

Figure 10 shows the taken IV-curves from a late 2023 manufactured cell, Figure 11 those of the mid-2024 cell. For better comparison the x-axis is the same. Both are M10 half cells with 16 busbars. It can be clearly seen that the reverse breakdown voltage is higher for the mid-2024 cell. However, compared to Al-BSF and PERC the reverse breakdown voltage is significantly higher, where the late 2023 has around −44V and the mid 2024 −48V.

The irradiance dependence is very low. To see at least some details the y-axis in Figures 10b and 11b are set to 2A vs. the 7A for PERC in Figure 7, noting that the short circuit current of the TOPCon cell (6.4/6.8A) is higher compared to the PERC cell (5.2A). Additionally the newer cell has a more sharp breakdown point compared to the older one.

That manufacturing processes can impact cell IV-characteristics is known e.g. from [35,36]. Figure 12 shows the IV-curves of three different M10 cells. Cell #1 and #3 were from the same batch and from mid 2024, #2 from late 2023. The reverse breakdown voltage varies from about −39V to −48V, which is quite a spread knowing that the cells came from the same cell box having same power and color sorting. Even that, the breakdown is still at a very

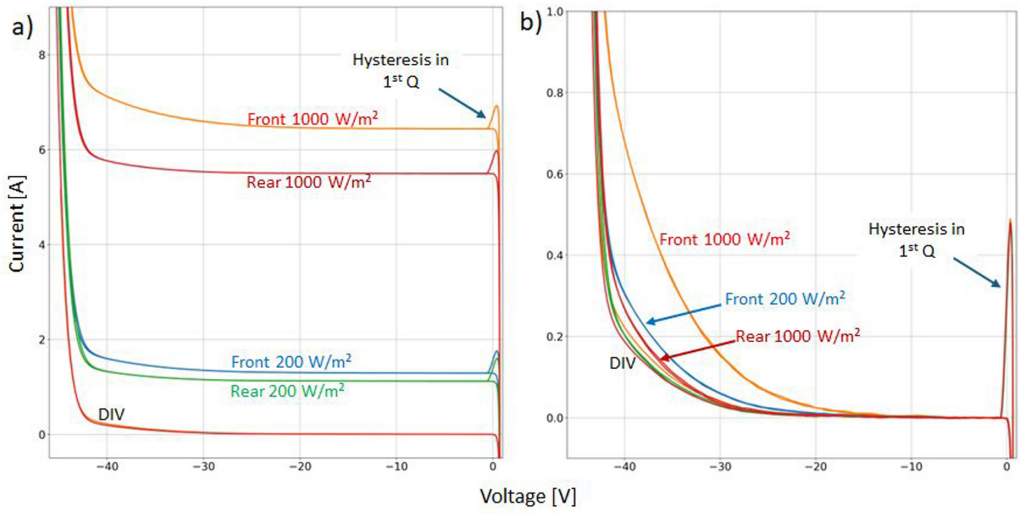

Fig. 9. IV-curves taken at 1000W/m^2, 200W/m^2 and in the dark are shown for the front and rear side of a TOPCon 16 busbar M10 cell in both Isc–> Voc and Voc –> Isc direction. a) The hysteresis in the 1st-quadrant is clearly visible due to the long IV-curve sweep required to measure to breakdown (appr. 85ms). There is no indication of a hysteresis effect at reverse breakdown as curves lay directly over each other. b) Same IV-curves but always moved by Isc of correlated intensity. On the front side a low irradiance dependence is visible at voltage above 20V.

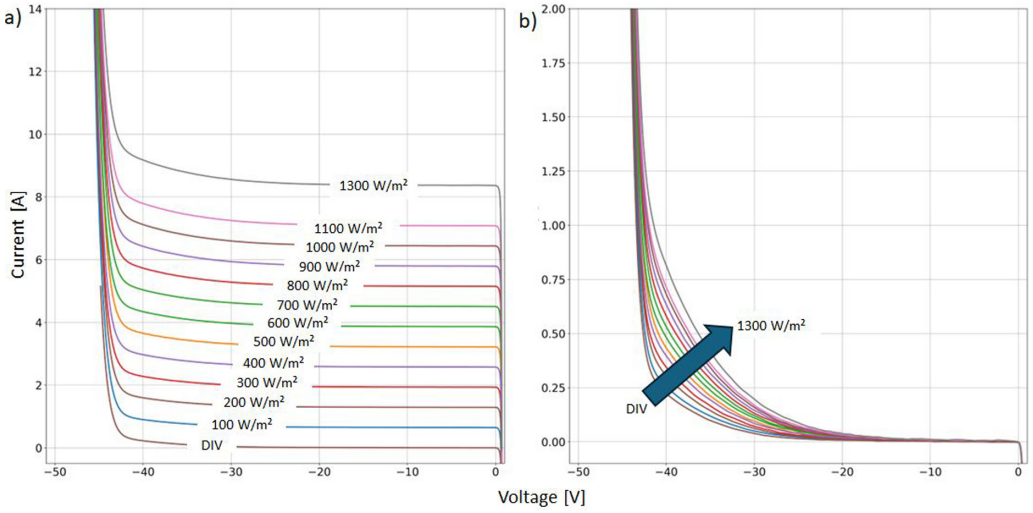

Fig. 10. a) IV-curves taken at 1300W/m^2 and from 1100W/m^2 to dark IV in 100W/m^2 steps of a 16 busbar TOPCon mono-crystalline half-cut cell from Figure 8, manufactured late 2023. b) same IV-curves but always moved by Isc of correlated intensity. Reverse breakdown occurs at around −44V significant higher compared to PERC and Al-BSF cells. There is almost no irradiance dependence visible, and please note the different, zoomed in y-axis scaling compared to PERC/Al-BSF.

high reverse voltage for cell #3 and most likely causing not an issue for hot-spots. It demonstrates the relevance of good metrology in the cell production factory as other effects may show another more severe impact on reverse breakdown voltage.

3.4 HJT cells

HJT cells are around for about two decades. However, never reached a significant market share. Recently, due to the potential of high efficiencies they got more interest and more manufacturers started production. Still the market share is low, mainly due to cost of the cell itself.

For this study a M6 half cut HJT cell type with 9 busbars was used (see Fig. 13). The EL-image shows some inhomogeneities that were a result of the sample manufacturing process, mainly in forming a good electric contact between ribbon and cell. Therefore the impact on solar cell IV-characteristic is very low, except a minor impact on serial contact resistance. It shows the expected strong hysteresis effect for fast IV-curve sweeps. Therefore, the reverse bias impact was also checked and no impact was found, similar to the TOPCon cells. As the HJT are also bifacial, front and rear side were separately checked. Both sides show same behavior. Compared to the TOPCon cells the bifaciality factor is, as expected, higher.

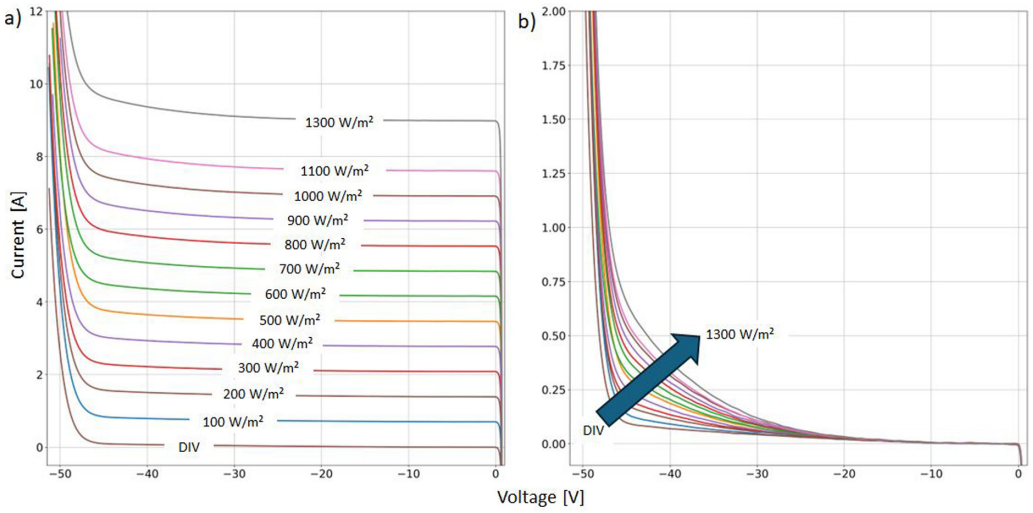

Fig. 11. a) IV-curves taken at 1300W/m^2 and from 1100W/m^2 to dark IV in 100W/m^2 steps of a 16 busbar TOPCon mono-crystalline half-cut cell from Figure 8, manufactured mid 2024. b) Same IV-curves but always moved by Isc of correlated intensity. Reverse breakdown occurs at around −48V slightly higher as the late 2023 TOPCon. There is a slightly more irradiance dependence visible compared to the late 2023 cell, resulting from a more sharp dark IV-curve breakdown point.

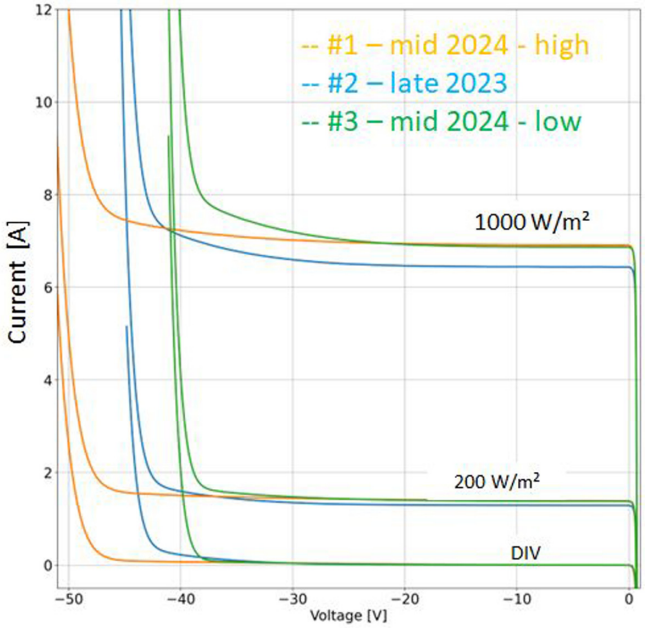

Fig. 12. a) IV-curves taken at 1000W/m^2, 200W/m^2 and dark IV for three different 16 busbar TOPCon G12 mono-crystalline half-cut cell. Two (#1 and #3) are from mid 2024 and also used in Figure 11, and one from late 2023 (#2) from Figure 10. A shift from around −48V to "only"-39V is clearly visible, showing the influence of manufacturing process. The lower current for #2 is mainly a result of different sample design with higher optical losses.

The measurement and the evaluation were done with the same procedure as for TOPCon described above. The results are shown in Figure 14.

From Figure 14 a reverse breakdown voltage of −30V was determined with basically no irradiance dependence. y-axis is same as for the TOPCon cells, the indicating arrow has the same length, but as x-axis is slightly different it is not fully same scaling, but still lower impact even compared to TOPCon.

3.5 IBC cells

The last cell in this study is IBC cell architecture. The main difference is that the contacts are both on the rear side, making this cell type very homogeneous on the front side and very interesting for aesthetically more pleasant PV modules. In the last few years more manufactures offer rear contacted cells with very high efficiencies. Their market share, even still small, grows [1].

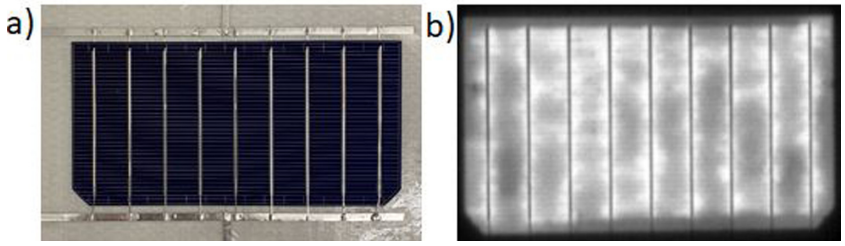

Fig. 13. HJT mono-crystalline silicon solar cell with 9 busbars manufactured in late 2023. a) photo of cells with contacts, b) corresponding EL-image showing some minor contacting issues between ribbons and cell.

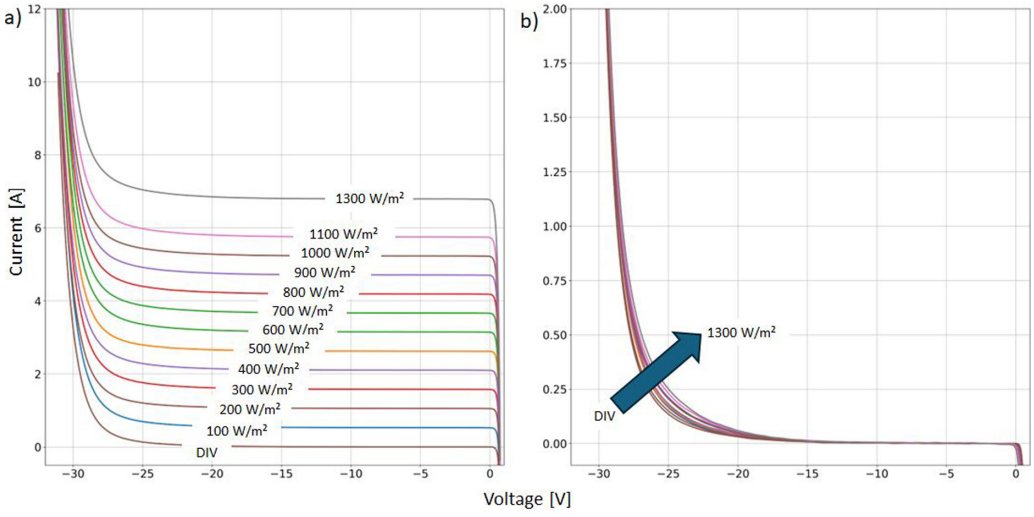

Fig. 14. a) IV-curves taken at 1300W/m^2 and from 1100W/m^2 to dark IV in 100W/m^2 steps of a 9 busbar HJT monocrystalline half-cut cell from Figures 13a, 13b. b) Same IV-curves but always moved by Isc of correlated intensity. Reverse-breakdown occurs at around −30V as known for that solar cell type. There is basically no irradiance dependence visible. The arrow is same length compared to Figures 10 and 11.

The cells in this study were 4 busbar R&D IBC cells. The EL-image did not show any major critical observations. Here also only a string of 8 cells was available and therefore the voltage was divided by number of cells to make plots comparable. It has to be mentioned that this measurement represents an average of the 8 cells, not a single cell measurement. The IV-curve processing was done the same way as for the other cells. The results are shown in Figure 15. The curves are basically aligned on top of each other. The little spread between −1 and −3V might be a result from the serial interconnection of the cells. The main difference compared to all other cells is that the breakdown occurs at around −4.5V, ten times smaller than TOPCon.

4 Discussion

The results from Section 3 are summarized in Table 1. Considering only the reverse breakdown voltages and assuming a fully shaded cell hot-spots are not likely to occur. Table 2 gives the maximum power in Watt (rev. break downvoltage * Isc) as reference and per cm^2 that can be dissipated by a certain number of given cells. W/cm^2 as base for comparison was used that all cell sizes can be put in one table as cells with M0, M3, M6 and M10 were used and absolute temperature will depend on available power per unit area. Thresholds were taken from the reverse breakdown voltage and considering the voltage each cell architecture can achieve in open circuit. Only for (multi-crystalline) Al-BSF with more than 24 cells in a string hot-spot heating can occur and agrees with the fact that such modules were typically not manufactured.

PERC, TOPCon and HJT have higher open circuit voltages compared to Al-BSF, but their reverse breakdown is also higher (partly because of the use of mono-crystalline material). Therefore, 24 cells for PERC and even 28 cells for TOPCon and HJT should be feasible from the reverse breakdown behavior under full shading. As full shading of a cell is very unlikely the detailed partial shading behavior must be studied to also cover other reliability impacting factors.

As IBC cells break down at very low voltages, in any configuration of more than 8 cells in series breakdown occurs if a cell in a string goes into reverse biasing. However, as breakdown voltage is very low, the available power per cm^2 is very small, resulting in no significant heating.

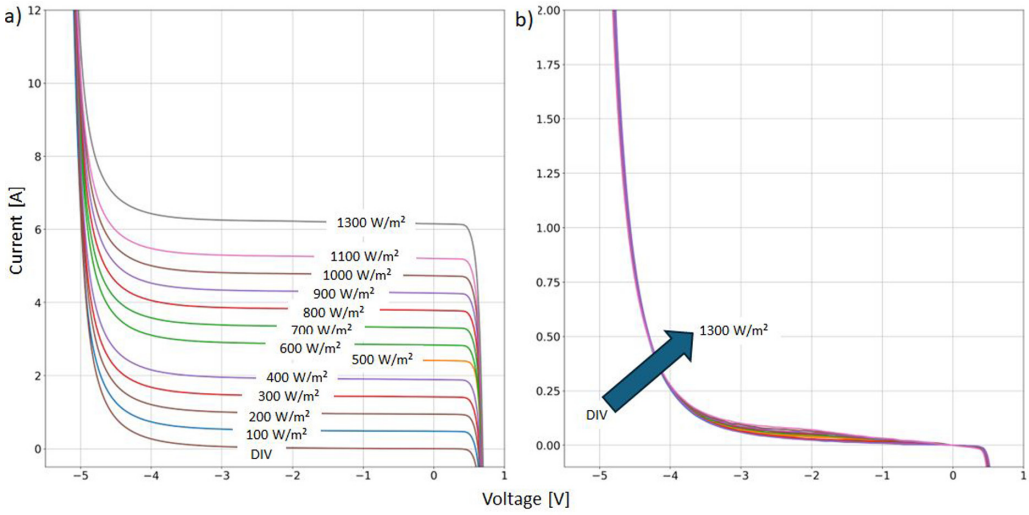

Fig. 15. a) IV-curves taken at 1300W/m^2 and from 1100W/m^2 to dark IV in 100W/m^2 steps of a IBC mono crystalline half-cut cell (voltage scaled by number of cells). b) Same IV-curves but always moved by Isc of correlated intensity. Reverse-breakdown occurs at around −4.5V as known for that solar cell type. There is basically no irradiance dependence visible. The arrow is same length compared to Figures 10, 11, and 14.

Table 1. Summary of parameters (size, Full cell (FC) vs Half cell (HC), and findings for the different cell architectures: Al-BSF, PERC, TOPCon, HJT and IBC). Cell sizes in brackets are available and stated for completeness, but not investigated. Irradiance dependence is qualitative measure.

#	Cell type	Typical size	FC / HC	Isc [A]	Voc [V]	Rev. breakdown [V]	Irr. dependence
1	Al-BSF	M0	FC	8.61	0.61	−14	Low
2	PERC	M3 M6 (M10, G12)	FC HC	9.11 5.20	0.67 0.67	−21 to −24	Strong
3	TOPCon	M10 (G12)	HC	6.44 6.87	0.72 0.73	−44 to −49 (lowest −39)	Low
4	HJT	M6 (M10, G12)	HC	5.19	0.73	−30	Very low
5	IBC	M3 (M6, M10, G12)	HC	4.77	0.68	−4 to −5	Very low

However, fully shaded cells in a PV module are a more rare occurrence. Partial shading is much more likely to occur. To account for this two contributions are considered: available charge carriers are set to the photo current of the partial shading scenario (50% of cell area shaded as worst-case; equals 50% Isc)) and an extra illumination enhanced reverse current at a given irradiance level (here 1000W/m^2). The extra currents for TOPCon and HJT are basically negligible, leading to basically no extra power for heating power as stated in Tables 3 and 4. As IBC break down at very low voltages breakdown always occur independent if 10 or 26 cells are interconnected in series (constant numbers).

However, for PERC and a little for Al-BSF the extra current for configurations of 20 or more cells per bypass diode is significant. The currents were determined from the graphs Figures 4,6,7 for each cell technology for 1000W/m^2 at the voltages for a given cell number can produce in open circuit. The extra irradiance dependent currents are given in Table 3.

From Table 3 the power for each configuration was calculated. Power is calculated from the assumption of 50% Isc plus an extra term from irradiance dependence (Tab. 3 Isc plus corresponding current form number of cells) multiplied by the available open circuit voltage from a particular number of cells in series. Cell size was considered and specific heat dissipation in W/cm^2 is given to make it cell dimensions independent (see Tab. 1). It was assumed that if breakdown occurs, the maximum voltage will be reverse breakdown voltage and not open circuit voltage of the string. This is why the numbers for 23 and 25 cells for Al-BSF and all numbers for IBC are identical. Numbers in W/cm^2 are doubled as heating is assumed to occur only in

Table 2. Maximum power for heating in [W] and per cm^2 [W/cm^2] assuming a fully shaded cell, reverse breakdown voltage and short circuit current as worse-case approximation. Corresponding cell sizes and parameters are given in Table 1.

Number of cells / cell type	**9**	**13**	**17**	**19**	**21**	**23**	**25**
Al-BSF	–	–	–	–	–	120 / 0.50	120 / 0.50
PERC	–	–	–	–	–	–	–
PERC	–	–	–	–	–	–	–
TOPCon	–	–	–	–	–	–	–
HJT	–	–	–	–	–	–	–
IBC	24 / 0.17	24 / 0.17	24 / 0.17	24 / 0.17	24 / 0.17	24 / 0.17	24 / 0.17

Table 3. Isc current for 50% cell and extra current due to illumination in reverse for different cell configurations, considering individual cell open circuit voltages. As irradiance dependence for TOPCon, HJT and IBC is low the current values are very small.

Number of cells / cell type	**Isc**	**9**	**13**	**17**	**19**	**21**	**23**	**25**
AlBSF	4.30	0	0.15	0.4	0.6	1	1.4	1.8
PERC	4.55	0	0.3	1	1.6	2.1	3	4
PERC	2.60	0	0.15	0.45	0.6	0.8	1.05	1.5
TOPCon	3.22	0	0	0	0	0	0.05	0.1
HJT	2.59	0	0	0	0	0	0.05	0.1
IBC	2.38	0.1	0.1	0.1	0.1	0.1	0.1	0.1

Table 4. Maximum power for heating in [W] and per cm^2 [W/cm^2] assuming a 50% (shaded cell) current. The red marked cells indicate full max power dissipation and limited by reverse breakdown voltage..

Number of cells / cell type	**9**	**13**	**17**	**19**	**21**	**23**	**25**
AlBSF	24 / 0.19	35 / 0.29	47 / 0.38	53 / 0.44	62 / 0.50	120 / 0.99 120 / 0.99	120 / 0.99 120 / 0.99
PERC	27 / 0.22	41 / 0.33	58 / 0.46	68 / 0.55	79 / 0.63	93 / 0.75	110 / 0.88
PERC	16 / 0.23	23 / 0.34	32 / 0.47	37 / 0.54	42 / 0.61	48 / 0.70	56 / 0.81
TOPCon	21 / 0.25	30 / 0.36	39 / 0.48	44 / 0.53	49 / 0.59	54 / 0.65	59 / 0.71
HJT	17 / 0.25	25 / 0.36	32 / 0.47	36 / 0.52	40 / 0.58	44 / 0.64	48 / 0.70
IBC	24 / 0.35	24 / 0.35	24 / 0.35	24 / 0.35	24 / 0.35	24 / 0.35	24 / 0.35

the non-shaded area. For the red marked configurations for Al-BSF this is most likely incorrect as it is known that shunting in such cells is often very localized e.g. due to bad edge-passivation or shunts in multi c-Si cells [8,10,34].

The shading scenario around 50% was found to be a worst-case for PERC [31,33]. The current model herein is simplified and superimposes two currents. That does not explain that low or high shading scenarios are not reaching maximum temperatures while the local current density in the non-shaded area is constant. The superposition must also have a voltage-dependent term that drives more current through the cell under partial shading as calculated here. This was also observed experimentally. Temperature and reverse bias drive more current through the cell (see also [32], generating most of the heat at around 50% shading. More research is needed here to better understand the process in detail.

5 Conclusions

In recent years crystalline solar cells developed significantly. With the technology advances efficiency was increased but also their IV-curve behavior was altered. In forward direction all classical IV-curve parameters improved. Current and voltages got higher, power increased together with the fill factor. These improvements lead to higher voltages in cell strings and also increase available power per unit area.

The results show for modern cells improved reverse breakdown voltages leading to basically hot-spot free modules under fully shaded cell conditions. Shades in real world conditions are typically different and only cover parts of a solar cell. A combination between active cell area and reverse breakdown result in localized heating of solar cells under partial shading. PERC technology shows the strongest dependence of the reverse bias illumination

current, leading to the most prone cell technology to show significant heating under partial shading. For a deeper understanding in the detailed mechanism on how and why such cells show under partial shading temperatures above 150°C further research is needed as for simulation multiple input parameters need to be considered such as shading scenario, irradiance level, number of strings in the circuit and heat transfer/generation from the unshaded solar cell area. TOPCon solar cells show the highest reverse breakdown voltage where breakdown occurs in the range from −39 to −49V, having a very large range for breakdown voltage pointing to changes in manufacturing processes. HJT cells show a reverse breakdown voltage at around −30V and PERC around −22V.

TOPCon and HJT cells are typically bifacial. Both show hysteresis effects for standard IV-curves but no hysteresis in the breakdown region. Front and rear side of the cells show the same reverse breakdown behavior under illumination.

To conclude, hot-spot heating due to partial shading may not be the biggest reliability issue to cause deterioration of the encapsulation system (encapsulate, front- and back-sheet) for TOPCon, HJT and IBC cell based PV modules even with 24 or 26 cells per bypass diode as power for heating is limited. For TOPCon and HJT the voltage from n−1 cells is well below reverse breakdown voltage whereas IBC cells break down at low voltages following a different "protection" path. Cells got significant larger in recent years (M3–> G12) and based on container dimensions the module size is now relatively fixed, the number of cells per bypass diode may decrease in the future considering current module design which would lead to lower voltages. However, it is known that these newer cell technologies themselves are more temperature sensitive (e.g. due to the use of low-temperature solder, special passivation layers) that even this extra heat generation is sufficient to cause cell degradation or a faster degradation of solder joints.

Shading will occur and partially shaded cells will have increased temperature. This is a fact and can't be fully mitigated, but temperature can be further lowered by decreasing the number of cells per bypass diode.

Another important topic for users is the loss of power due to partial shading. Dependent on the module internal circuitry and the PV system design, including IV-curve tracing of the inverter, the loss in energy yield due partial shading is higher with higher number of cells per bypass-diode. To limit the losses, shorter cell strings and more bypass diodes are more favorable.

Funding

This publication was funded by the Federal Ministry for Economic Affairs and Climate Action in the project SegmentPV under grant number 03EE1180. https://www.enargus.de/detail/?id=24059334 See Enargus: SegmentPV.

Conflicts of interest

There are no financial conflicts of interest. There are no specific trade names or similar used, except the reference to used equipment (HALM), which is given for clarity and completeness in the Experimental setup section.

Data availability statement

This article has no associated data generated and/or analyzed. No data is stored in public data repositories.

Author contribution statement

Bengt Jaeckel: Relevance of revisiting reverse bias, experiments, data analyse and paper writing. Jens Froebel: Sample preparation and experimental support. Matthias Pander: Discussion and review of paper. Andreas Maixner/Hamed Hanifi: Sample preparation, and discussions on module designs.

References

1. International Technology Roadmap for Photovoltaic (ITRPV), 15th Edition, 2024
2. J.W. Bishop, Computer simulation of the effects of electrical mismatches in photovoltaic cell interconnection circuits, Sol. Cells **25**, 73 (1988), https://doi.org/10.1016/0379-6787(88)90059-2
3. J.W. Bishop, Microplasma breakdown and hot-spots in silicon solar cells, Sol. Cells **26**, 335 (1989)
4. M. Danner, Reverse characteristics of commercial silicon solar cells-impact on hot spot temperatures and module integrity, in *Conference Record of the Twenty Sixth IEEE Photovoltaic Specialists Conference* (1997, IEEE, PVSC-97, 1997), pp. 1137–1140, https://doi.org/10.1109/pvsc.1997.654289
5. W. Herrmann, Hot spot investigations on PV modules-new concepts for a test standard and consequences for module design with respect to bypass diodes, in *IEEE Photovoltaic Specialists Conference* (1997), https://doi.org/10.1109/PVSC.1997.654287
6. W. Herrmann, *Operational behaviour of commercial solar cells under reverse biased conditions* (EU-PVSEC, 1998)
7. M.C. Alonso-Garcia, Analysis and modelling the reverse characteristic of photovoltaic cells, Sol. Energy Mater. Sol. Cells **90**, 1105 (2006)
8. D. Lausch, Identification of pre-breakdown mechanism of silicon solar cells at low reverse voltages, Appl. Phys. Lett. **97**, 073506 (2010)
9. C. Reichel, Investigation of electrical shading effects in back-contacted back-junction silicon solar cells using the two-dimensional charge collection probability and the reciprocity theorem, J. Appl. Phys. **109**, 024507 (2011), https://doi.org/10.1063/1.3524506
10. O. Breitenstein, Understanding junction breakdown in multicrystalline solar cells, J. Appl. Phys. **109**, 071101 (2011), https://doi.org/10.1063/1.3562200
11. H. Yang, Investigation of the relationship between reverse current of crystalline silicon solar cells and conduction of bypass diode, Int. J. Photoenergy **2012**, 1 (2012), https://doi.org/10.1155/2012/357218
12. K.A. Kim, Photovoltaic hot spot analysis for cells with various reverse-bias characteristics through electrical and thermal simulation, in *IEEE 14th Workshop on Control and Modeling for Power Electronics (COMPEL)* (IEEE, 2013), https://doi.org/10.1109/compel.2013.6626399
13. J. Qian, Two-dimensional hot spot temperature simulation for c-Si photovoltaic modules, Phys. Status Solidi A **215**, 1800429 (2018), https://doi.org/10.1002/pssa.201800429

14. IEC 61215-2, Crystalline silicon terrestrial photovoltaic (PV) modules − Design qualification and type approval (2016, 2022)
15. J. Wohlgemuth, Hot spot tests for crystalline silicon modules, in *IEEE Photovoltaic Specialists Conference* (2005)
16. S. Wendlandt, Hot spot risk analysis on silicon cell modulesâ, in *25th European Photovoltaic Solar Energy Conference and Exhibition* (EU-PVsec, 2010)
17. S. Wendlandt, *The temperature as the real hot spot risk factor at PV-modules* (EU-PVsec, 2012)
18. M. Garcia, Observed degradation in photovoltaic plants affected by hot-spots, Prog. Photovolt.: Res. Appl. **22**, 1292 (2013)
19. ST. Janke, *Comparison of hot spot endurance tests: temperature behavior of bare vs. encapsulated crystalline silicon cells* (EU-PVsec, 2014)
20. M. Sieg, *Schwarze schafe III: schmelzende rueckseitenfolien, kaputte zellen und hotspots* (Photovolaik, 2015)
21. S. Deng, Research on hot spot risk for high-efficiency solar module, Energy Procedia **130**, 77 (2017), https://doi.org/10.1016/j.egypro.2017.09.399
22. S.T. Wendlandt, *Advanced PV module hot spot characterization* (EU-PVsec, 2017)
23. B. Jaeckel, *Type approval and safety considerations for bifacial PV modules: requirements for IEC 6121 5 and IEC 61730* (EU-PVsec, 2018)
24. B. Jaeckel, Filling in the gaps: the evolution of high-density module design- technical possibilities and challenges (Webinar PV Magazine, 2020)
25. A. Mondon, *Comparison of layouts for shingled bifacial PV modules in terms of power output, cell-to-module ratio and bifaciality* (EU-PVSEC, 2018)
26. M. Lang, FEM simulation of deformations and stresses in strings of shingled solar cells under mechanical and thermal loading, in *AIP Conference Proceedings* (AIP Publishing, 2022), https://doi.org/10.1063/5.0126221
27. O. Kunz, Understanding partial shading effects in shingled PV modules, Sol. Energy **202**, 420 (2020), https://doi.org/10.1016/j.solener.2020.03.032
28. A. Tummalieh, Holistic analysis for mismatch losses in photovoltaic modules: assessing the impact of inhomogeneity from operational conditions and degradation mechanisms on power and yield, Prog. Photovolt.: Res. Appl. **34**, 39 (2024), https://doi.org/10.1002/pip.3865
29. Solar Power Europe, in *Global Market Outlook* (2024)
30. IEC TS 63126, Guidelines for qualifying PV modules, components and materials for operation at high temperatures, 2020, https://webstore.iec.ch/en/publication/59551
31. B. Jaeckel, *Hotspottest und reale teilverschattung von modernen high-density HD-modulen: eine wahrscheinlichkeits- und risikobetrachtung* (PV Symposium Bad Staffelstein, 2021)
32. E. Oezkalay, The effect of partial shading on the reliability of photovoltaic modules in the built-environment, EPJ Photovolt. **15**, 7 (2024), https://doi.org/10.1051/epjpv/2024001
33. R. Witteck, *Hot cells in high-power photovoltaic modules with solar cells from larger silicon wafer formats* (Eu-PVSEC, 2021), https://doi.org/10.4229/EUPVSEC20212021-4AV.1.25
34. J. Bauer, Hot spots in multicrystalline silicon solar cells: avalanche breakdown due to etch pits, Phys. Status Solidi (RRL) − Rapid Res. Lett. **3**, 40 (2009), https://doi.org/10.1002/pssr.200802250
35. F. Dauzou, Electrical behaviour of n-type silicon solar cells under reverse bias: Influence of the manufacturing process, Sol. Energy Mater. Sol. Cells **104**, 175 (2012), https://doi.org/10.1016/j.solmat.2012.04.046
36. V. Shanmugam, Impact of the manufacturing process on the reverse-bias characteristics of high-efficiency n-type bifacial silicon wafer solar cells, Sol. Energy Mater. Sol. Cells **191**, 117 (2019), https://doi.org/10.1016/j.solmat.2018.11.014
37. C. Clement, Illumination dependence of reverse leakage current in silicon solar cells, in *49th IEEE Photovoltaic Specialists Conference* (2021), Vol. 11, pp. 1285–1290, https://doi.org/10.1109/jphotov.2021.3088005
38. C. Clement, Design of shading- and hotspot-resistant shingled modules, Prog. Photovolt.: Res. Appl. **30**, 464 (2021), https://doi.org/10.1002/pip.3507
39. A. Kassis, Analysis of multi-crystalline silicon solar cells at low illumination levels using a modified two-diode model, Sol. Energy Mater. Sol. Cells **94**, 2108 (2010), https://doi.org/10.1016/j.solmat.2010.06.036
40. F. Khan, Effect of illumination intensity on cell parameters of a silicon solar cell, Sol. Energy Mater. Sol. Cells **94**, 1473 (2010), https://doi.org/10.1016/j.solmat.2010.03.018
41. E. Cuce, An experimental analysis of illumination intensity and temperature dependency of photovoltaic cell parameters, Appl. Energy **111**, 374 (2013), https://doi.org/10.1016/j.apenergy.2013.05.025
42. B. Jaeckel, Temperature dependence of reverse breakdown voltage onset of five cell technologies, to be published
43. VDE SPEC 90031 V1.0 (en), Electroluminescence (EL) of photovoltaic modules − terms and classification, 2025
44. B. Jaeckel, Nomenclature and description of Electro-Luminescence (EL) observations: cell cracks and other observations, EPJ Photovolt. **15**, 44 (2024), https://doi.org/10.1051/epjpv/2024039
45. P. Gebhardt, Reliability of commercial TOPCon PV modules-an extensive comparative study, Prog. Photovolt.: Res. Appl. **33**, 1378 (2024), https://doi.org/10.1002/pip.3868
46. F.T. Thome, UV-induced degradation of industrial PERC, TOPCon, and HJT solar cells: the next big reliability challenge? Sol. RRL **8**, 2400628 (2024), https://doi.org/10.1002/solr.202400628
47. P. Hacke, Enhancing lifetime, forecasting, and economic benefits of photovoltaic technologies undergoing UV-induced degradation with optical filtering, Jpn. J. Appl. Phys. **64**, 31 (2025), https://doi.org/10.35848/1347-4065/adbf29
48. A. Sinha, UV-induced degradation of high-efficiency silicon PV modules with different cell architectures, Prog. Photovolt.: Res. Appl. **31**, 36 (2022), https://doi.org/10.1002/pip.3606

Cite this article as: Bengt Jaeckel, Jens Froebel, Matthias Pander, Andreas Maixner, Hamed Hanifi, Characterization and analysis of reverse breakdown voltage onset of solar cells with different cell architectures, EPJ Photovoltaics 17, 4 (2026), https://doi.org/10.1051/epjpv/2025024